OXFORD

Mindfulness-Based Stress Reduction-related changes in posterior cingulate resting brain connectivity

Tammi R.A. Kral,[1,2,3] Ted Imhoff-Smith,[1] Douglas C. Dean, III[1,3]
Dan Grupe,[1,3] Nagesh Adluru,[1,3] Elena Patsenko,[1] Jeanette A. Mumford,[1,3]
Robin Goldman,[1,3] Melissa A. Rosenkranz,[1,3] and Richard J. Davidson[1,2,3,4,]

[1]Center for Healthy Minds, University of Wisconsin–Madison, Madison, WI 53703, USA, [2]Department of
Psychology, University of Wisconsin–Madison, Madison, WI 53703, USA, [3]Waisman Laboratory for Brain
Imaging and Behavior, University of Wisconsin–Madison, Madison, WI 53703, USA and [4]Department of
Psychiatry, University of Wisconsin–Madison, Madison, WI 53703, USA

Correspondence should be addressed to Richard J Davidson, Center for Healthy Minds, University of Wisconsin–Madison, 625 West Washington Avenue,
Madison, WI 53703, USA. E-mail: rjdavids@wisc.edu.

Abstract

Mindfulness meditation training has been shown to increase resting-state functional connectivity between nodes of the
frontoparietal executive control network (dorsolateral prefrontal cortex [DLPFC]) and the default mode network (posterior
cingulate cortex [PCC]). We investigated whether these effects generalized to a Mindfulness-Based Stress Reduction (MBSR)
course and tested for structural and behaviorally relevant consequences of change in connectivity. Healthy,
meditation-naïve adults were randomized to either MBSR ($N = 48$), an active ($N = 47$) or waitlist ($N = 45$) control group.
Participants completed behavioral testing, resting-state fMRI scans and diffusion tensor scans at pre-randomization (T1),
post-intervention (T2) and ∼5.5 months later (T3). We found increased T2–T1 PCC–DLPFC resting connectivity for MBSR
relative to control groups. Although these effects did not persist through long-term follow-up (T3–T1), MBSR participants
showed a significantly stronger relationship between days of practice (T1 to T3) and increased PCC–DLPFC resting
connectivity than participants in the active control group. Increased PCC–DLPFC resting connectivity in MBSR participants
was associated with increased microstructural connectivity of a white matter tract connecting these regions and increased
self-reported attention. These data show that MBSR increases PCC–DLPFC resting connectivity, which is related to increased
practice time, attention and structural connectivity.

Key words: mindfulness; resting-state connectivity; posterior cingulate; dorsolateral prefrontal cortex

Introduction

Mindfulness meditation practice aims to improve well-being
through training attention to present-moment experience
(Kabat-Zinn, 1990). There is growing evidence that mindfulness
meditation training improves multiple aspects of attention and

executive functioning, including improved working memory
(Zeidan *et al.*, 2010), decreased rumination and distraction
(Jain *et al.*, 2007) and decreased mind-wandering (Mrazek
et al., 2013). Moreover, decreases in mind-wandering mediated
improvements in cognitive performance following mindfulness
meditation training (Mrazek *et al.*, 2013). These behavioral

changes following mindfulness practice suggest dynamic alterations in brain networks responsible for implementing attention and executive function.

The posterior cingulate cortex (PCC) is the central hub of the default mode network (DMN; Spreng *et al.*, 2013), which is a set of brain regions in which activation is correlated at rest and is associated with mind-wandering and self-referential processing in task-based fMRI (Mason *et al.*, 2007; Andrews-Hanna *et al.*, 2010). A cross-sectional study of long-term mindfulness meditation practitioners by Brewer *et al.* (2011) found reduced activation of this network at rest and during meditation practice, which was interpreted as reflecting reduced mind-wandering and increased focus on present moment experience. However, research to date has not provided direct, supporting evidence for this interpretation. Brewer *et al.* (2011) also found increased resting-state functional connectivity (RSFC) between the PCC and a node of the frontoparietal executive control network (FPN), the dorsolateral prefrontal cortex (DLPFC), in long-term mindfulness practitioners compared to non-meditators, suggesting a functional mechanism by which attentional improvements and reductions in mind-wandering may manifest. The FPN coordinates activation between the DMN and the dorsal attention network, for example for top-down modulation of mind-wandering (MacDonald *et al.*, 2000; Smallwood *et al.*, 2012). Nodes of the FPN, including DLPFC, are also active during mind-wandering, and one interpretation infers this activation as constraining or regulating mind-wandering (Christoff *et al.*, 2009; Christoff *et al.*, 2016). A recent study found that PCC–DLPFC RSFC also increased following short-term mindfulness meditation training relative to an active control intervention (Creswell *et al.*, 2016).

Despite this progress, prior research is limited by small sample sizes, use of non-standard interventions, lack of meaningful behavioral correlates and failure to include diffusion-weighted measures of structural connectivity. In the present study we evaluated the impact of the most commonly used mindfulness intervention—Mindfulness-Based Stress Reduction (MBSR). MBSR is manualized, widely available and has been adapted for use in a variety of populations and contexts (Kabat-Zinn, 1990). Furthermore, arguments regarding the practical significance of mindfulness meditation-related changes in functional connectivity would be more compelling if these findings were mirrored by changes in the microstructure of pathways connecting these regions, and/or accompanied by alterations in behavioral processes served by these networks.

In the current study we sought to conceptually replicate and extend prior work showing that short-term mindfulness meditation training increases PCC–DLPFC RSFC in a randomized controlled trial of MBSR. We employed a validated, active control intervention well-matched to MBSR, the Health Enhancement Program (HEP) (MacCoon *et al.*, 2012), and utilized a sample size that was approximately double that used in prior research (Creswell *et al.*, 2016). We defined a PCC seed and PFC target region of interest (ROI) based on coordinates reported in Creswell *et al.* (2016); we refer to this region as 'LPFC', as these coordinates are anterior and ventral to the canonical DLPFC that is part of the FPN. We also investigated PCC connectivity with a more canonical, anatomically-defined DLPFC target ROI, the middle frontal gyrus (MFG; Petrides and Pandya, 1999; Kim *et al.*, 2012; Ptak, 2012) from the Harvard-Oxford Atlas (Craddock *et al.*, 2012). We examined individual differences in practice duration to determine whether there was a dosage effect on changes in RSFC. Finally, we investigated associations between increased PCC–DLPFC RSFC and decreased mind-wandering, and with microstructural connectivity of a white matter tract connecting PCC and DLPFC, the superior longitudinal fasciculus (SLF). Thus, the current study enables us to examine with rigorous design and methodology, the efficacy of mindfulness meditation training in altering the structure and function of brain circuits associated with mind-wandering and attention and their behavioral correlates.

Methods

This study is registered as a clinical trial with ClinicalTrials.gov (NCT02157766).

Participants

We recruited 140 healthy human participants (average age 44.3 ± 12.8 years; 83 female) from Madison, WI, and the surrounding community using flyers, online advertisements and advertisements in local media. Recruitment materials described the study as researching 'the impact of health wellness classes on the brain and body'. Sixteen participants had RSFC data excluded from baseline analysis due to excessive motion (described below; $n = 11$) or anatomical brain abnormalities as determined by a radiologist ($n = 5$). Participants were randomly assigned to one of three groups following baseline data collection: MBSR, the HEP active control group, or a waitlist control group (WL). Participants were block randomized following stratification based on gender (male and female) and age (25–39, 40–50 and 51–65 years). The intervention procedures were identical to those detailed by MacCoon *et al.* (2012). Twenty-nine additional participants were excluded from analysis of pre/post-differences: 16 participants withdrew prior to T2; 6 participants were excluded for failure to attend more than 1 HEP or MBSR class; 1 participant had poor data quality (severe signal dropout in PFC); 1 participant was excluded for medical reasons; and 5 participants were excluded due to excessive motion during the T2 scan. Thus, there were 31 MBSR (average age 41.4 ± 12.9 years; 18 female), 34 HEP (average age 43.6 ± 13.1 years; 22 female) and 30 WL (average age 43.0 ± 12.0 years; 19 female) participants in analyses of T2–T1 RSFC. An additional 10 participants withdrew prior to T3 and 3 were excluded for excessive motion at the third scan, resulting in 29 MBSR (average age 41.1 ± 13.5 years; 17 female), 27 HEP (average age 43.7 ± 13.4 years; 16 female) and 29 WL (average age 44.0 ± 11.7 years; 18 female) for T3–T1 RSFC analyses. A subset of participants completed the Emotional Styles Questionnaire (ESQ), which was introduced subsequent to the onset of data collection due to availability of the measure: 25 MBSR (average age 40.2 ± 12.5 years; 12 female), 24 HEP (average age 42.0 ± 13.5 years; 13 female) and 21 WL (average age 41.6 ± 10.6 years; 12 female).

Participants were excluded if any of the following applied, due to their potential impact on the current analyses or other aspects of the larger study in which they were enrolled: regular use of psychotropic or nervous system altering medication; psychiatric diagnosis in the past year or history of bipolar disorder, schizophrenia or schizoaffective disorder; color blindness; currently participating in another clinical trial; current asthma diagnosis; currently diagnosed with a sleep disorder or regularly taking prescribed sleeping medications; current night shift worker; significant training or practice in meditation or mind-body techniques such as yoga or Tai-Chi; expert in physical activity, music or nutrition (for HEP); any history of brain damage or seizures; medical problems that would affect the participant's ability to participate in study procedures. Written, informed consent was obtained from all participants according

to the Declaration of Helsinki (WMA, 2013) and the study was approved by the Health Sciences Institutional Review Board at the University of Wisconsin–Madison.

Data collection

Participants completed a baseline data collection visit prior to randomization, a second visit following the 8-week intervention period and a third visit ~5–6 months after the second visit. At each of these times, participants attended a 24 h laboratory visit that included an MRI scan and the ESQ (Kesebir *et al.*, n.d.) among other measures as part of a larger multisession, multiproject study. The ESQ consists of a 1–7 Likert scale with 1 = strongly disagree and 7 = strongly agree. One of the ESQ subscales provided a measure of attention that was most relevant to the hypotheses of the current study, and items included 'I do not get distracted easily, even when I am in a situation in which a lot is going on' and 'I sometimes feel like I have very little control over where my attention goes' (reverse-coded). Experimenters were blind to the group assignment during data collection. All participants were given monetary compensation for their participation.

Experience sampling

Experience Sampling was conducted during the week prior to and following the intervention period (14 days total). Participants provided their cellular phone numbers and available 8 h periods for each of the 14 days. Participants had a choice of receiving text messages six, seven or eight times a day, and received a text message every 90 min on average. The text message contained a question assessing mind-wandering: 'Was your attention on the activity you were performing?' Participants were asked to respond with a number from 1 (attention is not on the task) to 9 (attention is completely on the task at hand). On average participants responded to 82% of text messages they received. The response window was set to the time between two successive messages such that participants were given until the next message arrived to respond to the current message. If participants sent two responses in-between messages, the second response was discarded. The ratings across all 7 days of the week for each time period (pre/post-intervention) were averaged to obtain a mean attention rating for each participant at T1 and T2.

Image acquisition

Images were acquired on a GE MR750 3.0 Tesla MRI scanner with a 32-channel head coil. Anatomical scans consisted of a high-resolution 3D T1-weighted inversion recovery fast gradient echo image (450 ms inversion time; 256 × 256 in-plane resolution; 256 mm field of view (FOV); 192 × 1.0 mm axial slices). A 12 min functional resting-state scan run was acquired using a gradient echo echo-planar imaging (EPI) sequence (360 volumes; repetition time (TR)/echo time (TE)/Flip, 2000/20 ms/75°; 224 mm FOV; 64 × 64 matrix; 3.5 × 3.5 mm in-plane resolution; 44 interleaved sagittal slices; 3 mm slice thickness with 0.5 mm gap). The in-plane resolution was decreased after the first 21 participants from 3.5 × 3.5 to 2.33 × 3.5 mm to better address sinus-related artifacts, resulting in a matrix of 96 × 64. Diffusion-weighted images (DWIs) were acquired with single-shot spin-echo EPI sequence (TR/TE/Flip, 8575/76.6 ms/90°; 75 × 2 mm interleaved sagittal slices; 2.0 mm isotropic voxels). In total, 63 DWIs were acquired along non-collinear diffusion encoding directions across three *b*-values of 500/800/2000 s/mm^2 (9/18/36

directions, respectively), while six additional images with no diffusion encoding (i.e. *b* = 0 s/mm^2) were acquired. Parallel acquisition with a geometric reduction factor of two was used to reduce image acquisition time and distortions from magnetic field inhomogeneities. The total time for the multiple *b*-value DTI acquisition was 10 min.

Image processing: RSFC

Functional images were processed using a combination of AFNI (Cox, 1996) (versions 17.3) and FMRI Expert Analysis Tool Version 6.00, part of FMRIB's Software Library (FSL; Smith *et al.*, 2004), including the following steps: removal of the first four volumes, motion correction with MCFLIRT (Jenkinson *et al.*, 2002), BET (Smith, 2002) brain extraction and registration of the subject's functional data with their anatomical image using the boundary-based registration approach (Greve and Fischl, 2009). A 12 degrees of freedom (DOF) affine transformation using FLIRT (Jenkinson *et al.*, 2002) was followed by FNIRT nonlinear transformation to register each subject's functional data to Montreal Neurological Institute 152 space. Images were segmented into white matter, gray matter and cerebrospinal fluid with FAST for use as masks that were eroded using a 3 × 3 × 3 voxel kernel and then used to generate ROI-averaged time series serving as nuisance regressors (along with their derivatives and the six motion regressors) with AFNI's 3dDeconvolve. Images were smoothed with a 5 mm full-width half-maximum Gaussian kernel.

We extracted the time series from a spherical PCC seed with a 4 mm radius defined based on coordinates from Creswell *et al.* (2016). We regressed this time series back onto each subject's data using AFNI's 3dDeconvolve, which also censored high-motion time points (>0.2 mm framewise displacement; Power *et al.*, 2014). Participants were excluded from analysis if they had <6 min of data due to >50% of data points censored for motion. Two sets of target ROIs were defined: a bilateral DLPFC ROI, based on MFG from the Harvard-Oxford atlas (Craddock *et al.*, 2012) thresholded at 50% probability for small-volume-corrected voxelwise analysis, which was split into left and right for ROI analysis, and left and right LPFC ROIs defined as 10 mm spheres around coordinates provided in Creswell *et al.* (2016). Resting-state fMRI connectivity was assessed based on the Fisher-Z transformed (FZT) correlation between the PCC seed and every other voxel in the brain for the voxelwise analysis and separately for each of the target ROIs.

Image processing: DTI

DWIs were corrected for between-volume head motion and eddy currents using FSL's eddy tool (Andersson and Sotiropoulos, 2016), while diffusion encoding gradient directions were additionally corrected for rotations (Leemans and Jones, 2009). Brain extraction was performed using FSL's BET tool (Smith, 2002), and maps of diffusion tensors were calculated using the robust estimation of tensors by outlier rejection (Chang *et al.*, 2005) algorithm as implemented by the diffusion imaging in python open-source package (Garyfallidis *et al.*, 2014). Quantitative maps of functional anisotropy (FA), mean diffusivity (MD), radial diffusivity (RD) and axial diffusivity (AD) were derived from the diffusion tensors (Basser and Pierpaoli, 1996).

A population-specific template was created from a representative subset of the subject data to minimize coordinate system induced bias. Affine and diffeomorphic registration as imple-

mented in DTI-TK (Zhang *et al.*, 2006) were used for estimating the spatial transformations. Data from the individual subjects were spatially normalized to the estimated population-specific template. The Johns Hopkins University (JHU) ICBM-DTI-81 FA template (Mori *et al.*, 2005) was co-registered to our population-specific FA template using diffeomorphic registration as implemented by the Advanced Normalization Tools (Avants and Gee, 2004) software package. Deep white matter labels included as part of the JHU template were warped into the space of our population-specific template using nearest neighbor interpolation. Right and left hemisphere SLF ROIs were then inverse warped to the native space of each participant using the inverse of the subject-specific spatial transformation obtained from DTI-TK. Median FA, MD, RD and AD in these subject level SLF ROIs were then calculated. The median was used over the mean in order to be robust to outlier voxels within the ROIs.

Statistical analysis

The analysis plan for this study was pre-registered on the Open Science Framework at https://osf.io/vrmz9/register/5771ca429 ad5a1020de2872e. The analytic plan said linear models looking at T2 and T3 adjusting for T1 would be used, but we instead used T3–T1 and T2–T1 differences in our models, for consistency with analyses in other studies that were part of the larger project in which this study was embedded. We also changed the cutoff for the maximum number of TRs censored for motion from 25% to 50%, given that the resting-state scans were about twice as long in duration than those in prior studies on which this cutoff was defined. Analyses of baseline data regressed the T1 measures on group or other variables of interest. For each analysis examining changes due to MBSR, we computed difference scores (T2–T1 or T3–T1), which were regressed on group to test the effect of MBSR compared to HEP or to WL. Within-group analyses tested the intercept of the linear model for the difference score, reflecting whether or not the change in the dependent variable was significantly different than zero. Comparisons between two different variables regressed the difference score for one variable on the difference scores for the second variable. All tests were conducted using linear models from the "lm" function (for linear modeling) in the stats package in R (R Core Team, 2015). All analyses included covariates for age and gender, and analyses of RSFC included an additional covariate for the change in the resting-state scan acquisition (as described above). Significance of results were consistent regardless of inclusion of the covariates, except where noted in the text. All results are reported after removing outliers based on Cook's D, with a cutoff threshold of 4/(N-P) for data points disconnected from the distribution (where N = sample size and P = number of parameters in the model) as determined by the modelCaseAnalysis function of the lmSupport package (Curtin, 2015) in R (R Core Team, 2015). The significance of results is consistent with or without outliers included, except where indicated. We used a false discovery rate correction to control for multiple comparisons for each family of tests with the p.adjust function in the stats package in R (R Core Team, 2015), and the corrected *p*-values are indicated by $p*$.

RSFC analysis

In order to test for intervention effects, we computed difference maps for the T2 or T3 map subtracting the T1 map. We assessed the effects of mindfulness meditation on PCC–DLPFC RSFC by extracting the average RSFC FZT difference score across two sets of ROIs: (i) the anatomically-defined DLPFC ROI (split between left and right hemispheres of the Harvard-Oxford-defined MFG) and (ii) two spheres of 10 mm radius in left and right LPFC centered on coordinates provided by Creswell *et al.* (2016). The anatomical DLPFC ROIs provided a means to examine connectivity in a more 'canonical' DLPFC region than the spherical ROIs defined from Creswell *et al.* (2016) and were also broader than the spherical ROIs. In addition, we examined group differences in a voxelwise fashion within the DLPFC ROI. We conducted a secondary voxelwise analysis across the whole brain to identify other regions that might differ in connectivity between groups and to test for specificity of changes to PCC–DLPFC RSFC. Voxelwise analyses were thresholded at $P < 0.05$ controlling for familywise error (FWE) using threshold-free cluster enhancement with FSL's randomize (Winkler *et al.*, 2014).

Within the MBSR group, we tested relationships between PCC–DLPFC RSFC and two measures of mind-wandering as potential behaviorally relevant outcomes of stronger connectivity between these regions: self-reported attention on the ESQ (Kesebir et al., n.d.) and experience sampling of mind-wandering via text messaging. We included difference scores of the attentional measure as a covariate of interest for each participant in a voxelwise analysis within the anatomical DLPFC. We also examined this relationship in an ROI analysis by extracting the average PCC RSFC from the left and right anatomical DLPFC ROIs, which were entered as the independent variables in linear models with the attention measure (T2–T1 for both variables).

DTI analysis

We tested whether MBSR-related changes in PCC–DLPFC RSFC were associated with changes in the SLF using DTI measures. The median values for FA, MD, RD and AD of the SLF ROIs were entered into a principle component analysis (PCA; Zeestraten *et al.*, 2016; McLaughlin *et al.*, 2018), using the prcomp function in R (R Core Team, 2015) to construct a right and left hemisphere composite of the underlying microstructure. The first principle component was used as a representative composite of white matter microstructure, as this accounted for the greatest covariance between the four DTI parameters (77.1% for the right and 80.0% for the left). The factor loadings for FA, RD, MD and AD were 0.44, −0.54, −0.56 and −0.45 for the right side, respectively; and 0.45, −0.53, −0.56 and −0.46 for the left side, respectively. Thus, larger values of the microstructure composite are indicative of higher anisotropy and lower diffusivity, which is generally interpreted as a superior white matter microstructure (Basser and Jones, 2002; Jones *et al.*, 2013). DTI values at T2 were computed using the weights from this first principle component of the PCA analysis using the predict function in R (R Core Team, 2015).

Results: confirmatory analyses

Group differences in PCC RSFC

ROI analysis. Using anatomically generated DLPFC ROIs, participants who completed MBSR had increased PCC-right DLPFC RSFC from pre- to post-intervention compared to participants who completed HEP [$t(59) = 2.16$; $P = 0.04$; $P* = 0.05$; $b = 0.05$; confidence interval (CI) = (0.004, 0.10); 1 HEP outlier removed] and compared to WL [$t(55) = 2.53$; $P = 0.01$; $P* = 0.04$; $b = 0.06$; CI = (0.01, 0.10); 1 WL outlier removed; Figure 1A]. Post-hoc analyses revealed that the change in PCC–DLPFC RSFC was significantly positive for MBSR [$t(27) = 3.66$; $P = 0.001$; $P* = 0.003$; $b = 0.05$; CI = (0.02, 0.08)] and non-significant for HEP [$t(29) = 0.05$;
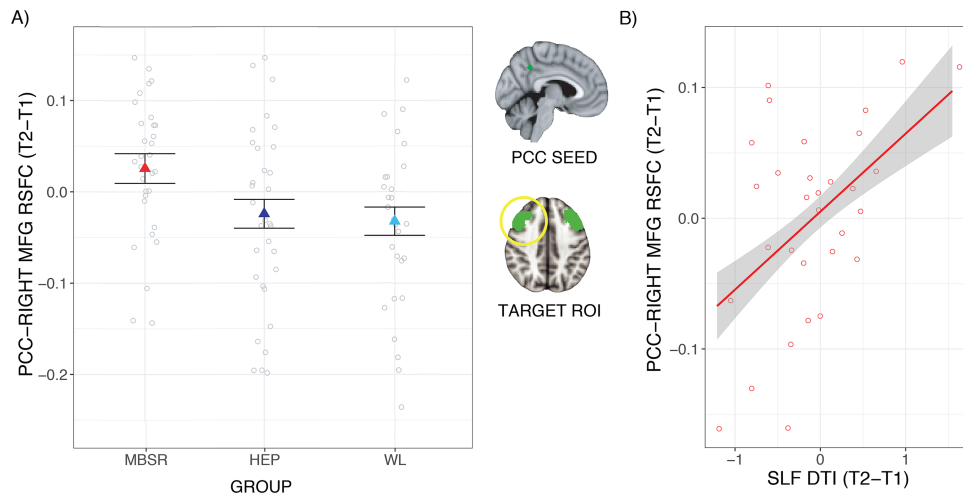
Fig. 1. MBSR-related changes in PCC–DLPFC RSFC: ROI results. **(A)** Participants had increased PCC–DLPFC RSFC (time 2–time 1) following MBSR compared to HEP and compared to WL. The PCC seed ROI and the anatomical DLPFC target ROIs are depicted in green with the right DLPFC circled in yellow. **(B)** A larger increase in MBSR participants' PCC–right DLPFC RSFC was associated with a larger increase in DTI integrity of a white matter tract connecting these regions (SLF) from pre- to post-intervention. Error bars/envelopes represent 1 standard error above and below the point estimates of the means, and raw data points are overlaid.
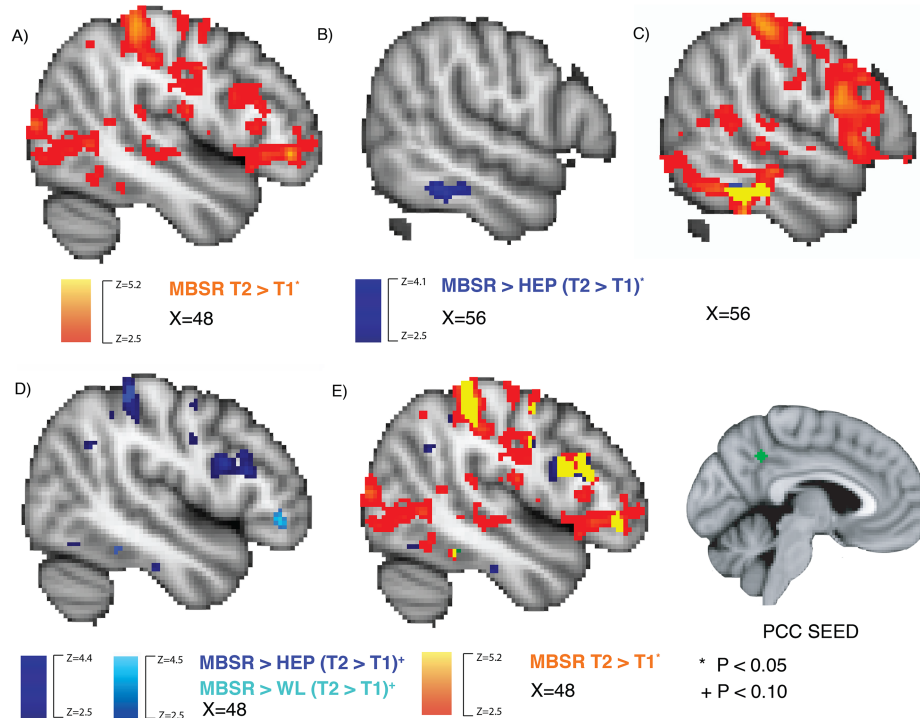

Fig. 2. MBSR-related changes in PCC RSFC: voxelwise results. The PCC seed is inset in the lower right in green. **(A)** Brain regions where MBSR participants had increased PCC RSFC (time 2–time 1) are depicted in yellow-orange ($P < 0.05$ controlling for FWE using threshold-free cluster enhancement with FSL's randomize). **(B)** The significant group difference between MBSR and HEP. **(C)** The overlap between A and B is depicted in yellow. **(D)** The marginal group differences for MBSR compared to HEP or WL are depicted in dark and light blue, respectively ($P < 0.10$ corrected). **(E)** The overlap between panels C and D is depicted in yellow.

$P = 0.96$; $P^* = 0.96$; $b = 0.001$; CI $= (-0.04, 0.04)$; 1 outlier removed] and WL [$t(25) = -0.25$; $P = 0.81$; $P^* = 0.96$; $b < -0.01$; CI $= (-0.04, 0.03)$; 1 outlier removed]. The difference in PCC connectivity with left DLPFC was significant for MBSR compared to HEP [$t(60) = 2.13$; $P = 0.04$; $P^* = 0.05$; $b = 0.06$; CI $= (0.003, 0.11)$] but non-significant compared to WL [$t(52) = 1.34$; $P = 0.19$; $P^* = 0.19$; $b = 0.03$; CI $= (-0.02, 0.08)$; 2 WL and 2 MBSR outliers removed]. There were no group differences in PCC–DLPFC RSFC at baseline for MBSR relative to HEP or WL in either hemisphere ($ts < -1.77$ and $Ps > 0.10$).

We tested whether changes in PCC–DLPFC RSFC persisted to T3. There were no significant group differences in T3–T1 PCC–DLPFC RSFC for MBSR compared to HEP [right DLPFC: $t(50) = 0.99$, $P = 0.33$, $P^* = 0.44$, $b = 0.03$, CI $= (-0.03, 0.08)$, 1 HEP outlier removed; left DLPFC: $t(50) = 1.06$, $P = 0.30$, $P^* = 0.44$, $b = 0.03$, CI $= (-0.03, 0.08)$, 1 HEP outlier removed]. There were also no group differences in T3–T1 PCC–DLPFC RSFC for MBSR *vs* WL [right DLPFC: $t(52) = 1.12$, $P = 0.27$, $P^* = 0.44$, $b = 0.03$, CI $= (-0.02, 0.08)$, 1 WL outlier removed; left DLPFC: $t(53) = 0.54$, $P = 0.60$, $P^* = 0.60$, $b = 0.02$, CI $= (-0.04, 0.07)$].

Table 1. MBSR-related increases in PCC RSFC: cluster details (100 voxel minimum)

	Region	Peak coordinates			Volume (voxels)
		X	Y	Z	
MBSR vs HEP* (T2–T1)	Right inferior temporal gyrus (P < 0.05)	56	−40	−18	218
	Right supramarginal gyrus	52	−34	58	3746
	Right inferior temporal gyrus	56	−40	−18	1849
	Left postcentral gyrus	−36	−32	50	941
	Right IFG	44	12	20	826
	Right supplementary motor cortex	4	8	58	217
	Left precentral gyrus	−36	4	22	130
	Left inferior temporal gyrus	−46	−56	−12	123
MBSR vs WL * (T2–T1)	Right anterior cingulate gyrus	8	−8	34	968
	Left precentral gyrus	−36	4	22	299
	Left insula	−42	2	0	271
	Right postcentral gyrus	24	−32	42	231
	Left inferior frontal gyrus	−50	32	10	134
	Left insula	−36	4	−16	109
	Right middle temporal gyrus	60	−24	−14	102
MBSR (T2-T1)	Right postcentral gyrus	50	−32	56	25 200
	Left middle temporal gyrus	−42	−60	−10	769
	Left putamen	−30	2	8	197
	Left fusiform cortex	−18	−76	−14	160

*Clusters for MBSR relative to control groups were marginal and non-significant with FWE cluster correction at P < 0.10 except in one case as noted, and change within MBSR was significant corrected at P < 0.05.

Using ROIs generated from coordinates in Creswell *et al.* (2016), there were no group differences in PCC–LPFC RSFC for T2–T1 for MBSR compared to HEP [right LPFC: $t(55) = −0.19$, $P = 0.85$, $P* = 0.94$, $b = −0.01$, CI = (−0.07, 0.05), 1 MBSR and 4 HEP outliers removed; left LPFC: $t(59) = −0.08$, $P = 0.94$, $P* = 0.94$, $b = −0.002$, CI = (−0.06, 0.05); 1 HEP outlier removed]. There were also no group differences in PCC–LPFC RSFC connectivity from T1 to T2 for MBSR compared to WL [right LPFC: $t(56) = 1.50$, $P = 0.14$, $P* = 0.56$, $b = 0.05$, CI = (−0.02, 0.11); left LPFC: $t(54) = −0.63$, $P = 0.53$, $P* = 0.94$, $b = −0.02$, CI = (−0.07, 0.00); 2 WL outliers removed]. Given that the effects of MBSR training were limited to PCC RSFC with the anatomically defined DLPFC, subsequent analyses were limited to examining PCC RSFC with this target ROI.

Voxelwise analysis. There were no regions in which PCC RSFC differed for MBSR participants compared to HEP or WL at baseline in the whole-brain analysis. MBSR participants showed significant increases in PCC RSFC with a network of regions that included DLPFC [primarily inferior frontal gyrus (IFG)] from T1 to T2 in the voxelwise, whole-brain analysis (Figure 2A). MBSR participants had significantly increased PCC RSFC with a region in right inferior temporal gyrus (ITG) compared to HEP (Figure 2B) and no significant differences compared to WL. No statistically significant differences were observed in PCC–DLPFC RSFC when comparing MBSR to control groups in the wholebrain, voxelwise analysis. However, at a whole-brain threshold of P < 0.10, MBSR participants had increased PCC RSFC with right DLPFC (primarily IFG) relative to HEP and with left frontal pole relative to WL (Figure 1C and D), among other regions (see Table 1 for detailed cluster information). There were no regions with significant (or marginal) changes in PCC RSFC within HEP or WL, and no regions where HEP or WL increased in PCC RSFC relative to MBSR (either significantly or at a trend level).

MBSR participants had increased PCC RSFC with right DLPFC in the small-volume-corrected, voxelwise analysis (Figure 3A). No significant group differences were observed in the voxelwise analysis restricted to the anatomical DLPFC ROI when comparing MBSR to control groups. However, at a threshold of P < 0.10, MBSR participants had increased PCC RSFC with right DLPFC relative to HEP (Figure 3B). We observed the same pattern for MBSR compared to WL; however, at baseline WL participants also had higher PCC RSFC than MBSR participants in an overlapping cluster of right DLPFC (Figure 3C). There was no difference in PCC–DLPFC RSFC between MBSR and HEP at baseline.

There were no regions across the whole brain or within the small-volume-corrected anatomical DLPFC that showed significant group differences in PCC RSFC from T1 to T3.

Experience sampling

Within the MBSR group, there was no significant relationship between changes in PCC–DLPFC RSFC and mind-wandering based on experience sampling in the voxelwise analysis (P < 0.05 corrected for FWE), nor in the ROI analyses [right DLPFC: $t(21) = −1.12$, $P = 0.28$, $P* = 0.28$, $b = −2.24$, CI = (−6.43, 1.95), 1 outlier removed; left DLPFC: $t(21) = −1.95$, $P = 0.07$, $P* = 0.14$, $b = −2.62$, CI = (−5.42, 0.18), 1 outlier removed]. There was no difference in the change in mind-wandering between MBSR and HEP [$t(62) = 0.85$, $P = 0.40$, $P* = 0.40$, $b = 0.17$, CI = (−0.24, 0.58), 1 HEP and 1 MBSR outlier removed] or WL [$t(73) = 1.91$, $P = 0.06$, $P* = 0.12$, $b = 0.31$, CI = (−0.01, 0.64), 1 MBSR outlier removed].

Results: exploratory analyses

Structural connectivity

There were no group differences between the change in SLF DTI for MBSR compared to HEP [right SLF: $t(70) = 0.08$, $P = 0.94$, $P* = 0.94$, $b = 0.01$, CI = (−0.21, 0.23), 4 MBSR outliers removed; left
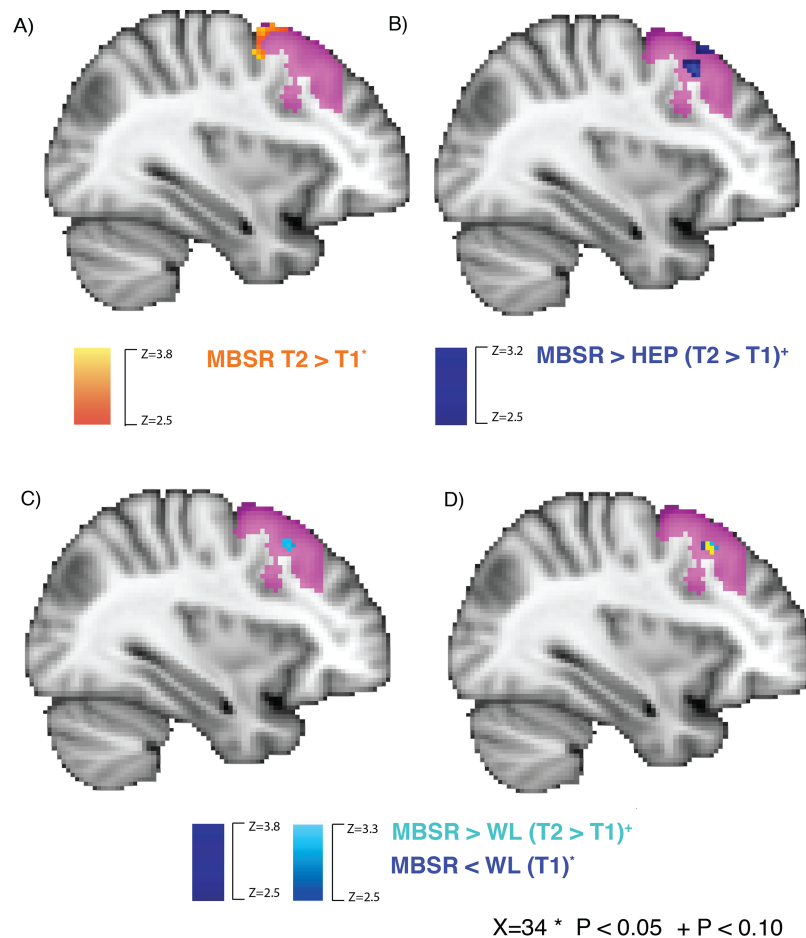
Fig. 3. MBSR-related changes in PCC–DLPFC RSFC: voxelwise results. **(A)** MBSR participants had increased PCC RSFC (time 2–time 1) (*P* < 0.05, controlling for FWE using threshold-free cluster enhancement with FSL's randomize). **(B)** The marginal group difference for MBSR compared to HEP (*P* < 0.10, corrected). **(C)** The marginal group differences for MBSR compared to WL (*P* < 0.10, corrected). **(D)** The overlap between C and time 1 differences (dark blue; *P* < 0.05, corrected) between MBSR and WL is depicted in yellow.

SLF: *t*(73) = 0.94, *P* = 0.35, *P** = 0.47, *b* = 0.10, CI = (−0.11, 0.31), 1 MBSR outlier removed] or compared to WL [right SLF: *t*(74) = 0.94, *P* = 0.35, *P** = 0.47, *b* = 0.13, CI = (−0.14, 0.40); left SLF: *t*(72) = −1.31, *P* = 0.20, *P** = 0.47, *b* = −0.14, CI = (−0.35, 0.07), 1 WL and 1 MBSR outlier removed]. However, within the MBSR group, increased PCC–right DLPFC RSFC was associated with increased SLF DTI from T1 to T2 [*t*(26) = 2.93; *P* = 0.01; *P** = 0.02; *b* = 0.06; CI = (0.02, 0.11); Figure 1B]. There was no relationship in the MBSR group with change in PCC–DLPFC RSFC and SLF DTI on the left side [*t*(25) = 1.00; *P* = 0.33; *P** = 0.33; *b* = 0.05, CI = (−0.05, 0.15); 1 outlier removed].

Practice time

The change in PCC–left DLPFC RSFC from pre- to post-intervention was associated with practice time to a significantly higher degree in MBSR relative to HEP on the left side [*t*(57) = 2.22; *P* = 0.03; *P** = 0.06; *b* = 0.004; CI = (0.0004, 0.01); 1 MBSR outlier removed; Figure 4A]; however, this relationship was non-significant when the influential outlier was included [*t*(58) = 1.59; *P* = 0.12; *P** = 0.24; *b* = 0.003; CI = (−0.001, 0.01)]. Within the MBSR group the relationship between practice and PCC–left DLPFC RSFC was significantly positive [*t*(25) = 2.12; *P* = 0.04; *P** = 0.08; *b* = 0.003; CI = (0.0001, 0.01); 1 MBSR outlier removed], whereas there was no relationship for HEP [*t*(29) = −0.67; *P* = 0.51; *P** = 0.51;

b = −0.001; CI = (−0.003, 0.002)]. The group difference in the relationship was non-significant on the right side [*t*(55) = 0.69; *P* = 0.49; *P** = 0.49; *b* = 0.001 CI = (−0.002, 0.004); 3 HEP outliers removed].

There was no significant group difference in the relationship between practice and PCC–left DLPFC RSFC at T3 [*t*(47) = 0.17; *P* = 0.17; *P** = 0.17; *b* < 0.01; CI = (−0.0003, 0.001); 1 MBSR and 1 HEP outlier removed]. The change in PCC–right DLPFC RSFC from T1 to T3 was associated with practice over the same time period to a significantly higher degree in MBSR compared to HEP [*t*(47) = 2.34; *P* = 0.02; *P** = 0.04; *b* = 0.001; CI = (<0.001, 0.002); 2 HEP outliers removed; Figure 4B].

Attention questionnaire

Increased self-reported attention on the ESQ was associated with stronger PCC–left DLPFC RSFC from pre- to post-MBSR (T2–T1) in the voxelwise analysis, *P* < 0.05 corrected for FWE (Figure 5). There was no significant association between change in ESQ attention and PCC RSFC with the right [*t*(20) = −0.70; *P* = 0.49; *P** = 0.49; *b* = −1.05; CI = (−4.18, 2.08); 1 outlier removed] or left DLPFC [*t*(19) = 1.09; *P* = 0.34; *P** = 0.49; *b* = 1.08; CI = (−1.22, 3.40); 2 outliers removed] in the ROI analysis. There was no group difference in the change in self-reported attention between MBSR
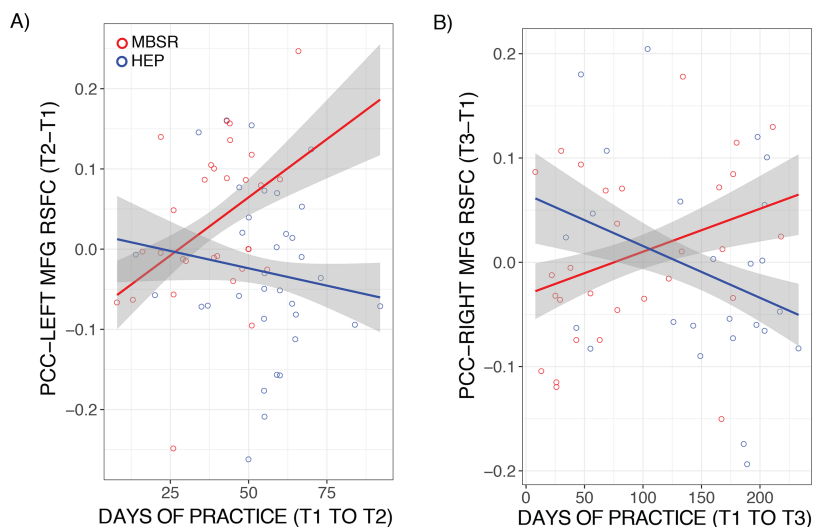
Fig. 4. Effects of MBSR practice duration. **(A)** MBSR participants had stronger PCC–DLPFC RSFC with more total days of practice compared to HEP between T2 and T1 for the left DLPFC and **(B)** T3 and T1 for the right DLPFC. Envelopes represent 1 standard error above and below the point estimates of the means, and raw data points are overlaid.
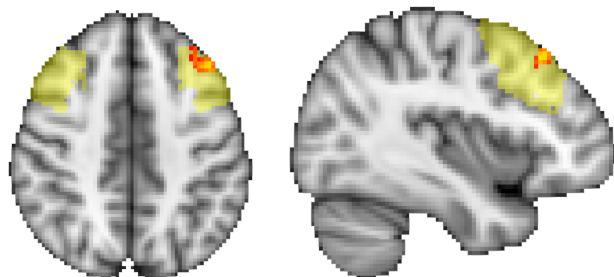

Fig. 5. MBSR-related increased PCC–DLPFC RSFC and attention. The more participants' PCC–left DLPFC RSFC increased (time 2–time 1) following MBSR, the more their self-reported attention also increased (red-yellow; $P < 0.05$ controlling for FWE using threshold-free cluster enhancement with FSL's randomize). The anatomical DLPFC ROI is underlaid in light yellow.

and HEP [$t(54) = 1.21$; $P = 0.23$; $P^* = 0.23$; $b = 0.18$; CI = (−0.12, 0.49)] or WL [$t(58) = 1.41$; $P = 0.16$; $P^* = 0.23$; $b = 0.23$; CI = (−0.10, 0.55)].

Discussion

In this study we found evidence that MBSR—one of the most widely used mindfulness meditation interventions—increased RSFC between nodes of the DMN and the FPN compared to well-matched active and passive control groups. Previous research has found similar effects following a brief mindfulness intervention relative to relaxation training (Creswell *et al.*, 2016), as well as in cross-sectional research of long-term practitioners (Brewer *et al.*, 2011). A large and growing body of research has implicated the DMN in mind-wandering, task-unrelated thought and self-referential processing, whereas the FPN is associated with externally-oriented and goal-directed attention (Spreng and Grady, 2009; Barrett and Satpute, 2013; Spreng *et al.*, 2013). Given that one of the primary skills trained during mindfulness meditation is directing attention to present moment experience without elaboration (unlike during typical self-referential processing), increased PCC–DLPFC RSFC could reflect a greater ability to attend to task-related stimuli and increased control over self-referential processing and mind-wandering.

The group differences in RSFC were localized to MFG, which is a more canonical region of the DLPFC (and of the FPN; Petrides and Pandya, 1999; Kim *et al.*, 2012; Ptak, 2012) that is posterior and dorsal to the regions reported by Creswell *et al.* (2016). In contrast, we failed to replicate prior findings using an ROI based on the exact coordinates provided by this prior study. There is a growing body of evidence suggesting the anatomically-defined DLPFC region should be involved in attentional processes that shift with mindfulness training (Fox *et al.*, 2016), whereas the LPFC ROI is based on coordinates from a single study and is likely less reliable. Although there were no significant group differences in PCC–DLPFC RSFC in the voxelwise analyses, we report the subthreshold results given that the pattern is consistent with the significant group difference in the anatomical DLPFC ROI analysis, and to provide a complete picture of the data. However, subthreshold results alone are not evidence of a group difference, given the possibility of false positives. The significant increase in PCC–DLPFC RSFC within MBSR participants in the voxelwise analyses adds further evidence to this pattern of results implicating MBSR practice with improved connectivity between the DMN and FPN.

There was an unanticipated, significant group difference in the voxelwise analysis, whereby MBSR participants had increased PCC–ITG RSFC relative to HEP. While there was no difference between MBSR and WL in PCC–ITG RSFC, this result appears to be driven by the significant increase for the MBSR group, as there was no change for HEP (or WL). The ITG has been considered part of the FPN (Kim *et al.*, 2012), and reduced ITG RSFC has been associated with aging-related cognitive impairment (Han *et al.*, 2011; Agosta *et al.*, 2012). Increased PCC–ITG RSFC may therefore reflect improved cognitive function. However, future research is needed to replicate this finding in a confirmatory analysis.

Importantly, we also found a group difference in the relationship between practice and change in PCC–DLPFC RSFC, whereby it was stronger for MBSR relative to HEP. The more time participants spent practicing MBSR, the stronger their PCC–left DLPFC RSFC became—representing a linear dosage effect at this early stage of training. There was no significant relationship for HEP practice and PCC–DLPFC RSFC. Since participants in the MBSR

group did not all engage to the same degree with practicing mindfulness meditation, the intervention should not lead to an equivalent change across MBSR participants as a group. This interaction of an individual differences measure with group is strong evidence that MBSR practice played a causal role in the RSFC changes, particularly given the significant main effect of group on change in PCC–DLPFC RSFC.

While the group difference in changes in brain connectivity was not sustained at the later follow-up, continued practice with MBSR may be necessary to maintain this effect. Our finding that days of MBSR practice between T1 and T3 were positively associated with increasing strength of RSFC of this network over the same time period adds support to this hypothesis. Future research should seek to replicate this effect since it was not pre-registered in this study, and to examine whether individuals who continue to practice mindfulness meditation following MBSR and incorporate the practices into their daily lives experience more lasting change. For example, future studies may extend this line of research by following participants further out in time and examining whether participants engage in mindfulness practices when dealing with stressors *vs* solely as a sitting practice.

Increased PCC–DLPFC RSFC following MBSR training was associated with increased white matter microstructure of a tract linking these regions, the SLF, in an exploratory analysis. Decreased diffusivity and increased fractional anisotropy in white matter may reflect a more streamlined white matter fiber organization (Beaulieu, 2002; Alexander *et al.*, 2007; Zatorre *et al.*, 2012). However, changes in DTI-based measures are non-specific and may stem from various alterations to the underlying microstructure (Jones and Cercignani, 2010; Jones *et al.*, 2013). Thus, the cellular and molecular mechanisms underlying such changes still require future investigation. While the white matter microstructure of the entire group of MBSR participants' SLF did not change significantly following the intervention, our findings highlight the importance of examining individual differences, since it was only for those who showed more substantial changes in functional connectivity that we observed alterations in white matter structural connectivity. Future research should examine relationships between structural and functional connectivity in this network in a confirmatory manner to replicate these findings.

While we also found an association between increased PCC–DLPFC RSFC and self-reported attention, as theorized, the relationship was only present in an exploratory analysis with a different measure than hypothesized in our pre-registration. The questionnaire measure utilized in the current study (ESQ) is also new, and the nomological network associated with individual differences on this measure remains to be determined. It will be important for future research to conceptually replicate this result with a validated ESQ or other validated self-report measure. Moreover, there was no relationship between changes in PCC–DLPFC RSFC and mind-wandering as measured by experience sampling following MBSR, contrary to our hypothesis. It is possible that the experience sampling measure in the current study assays a different aspect of attention than that which is supported by PCC–DLPFC connectivity, and/or that this measure is insufficient for measuring MBSR training-related changes. It is critical to identify behavioral measures associated with MBSR-related increases in PCC–DLPFC RSFC in order to more fully understand the relevance of such changes in brain connectivity. The ideal test would identify behavioral improvements following MBSR that are mediated by increased PCC–DLPFC RSFC.

Limitations

In the current study we found a mixture of positive and negative results, across confirmatory and exploratory analyses. Strong conclusions regarding the effect of MBSR training on PCC–DLPFC RSFC are limited, given that group differences in the voxel-wise analysis were non-significant and the *P*-values of the ROI analyses change from 0.04 to 0.05 in two cases when correcting for multiple comparisons. While our pre-registered analysis of the *a priori* anatomical ROIs provide support for the conclusion that MBSR strengthens PCC–DLPFC RSFC, further research is needed to replicate these effects. Replication of the results of multiple exploratory analyses is also needed, including relationships with practice, structural change of the SLF and increased self-reported attention. Moreover, the questionnaire measure we utilized (ESQ) remains to be validated. Finally, results of the whole-brain analysis revealed an unanticipated difference in PCC–ITG RSFC between MBSR and HEP that was non-significant for MBSR compared to WL. Since this group difference in PCC–ITG RSFC was the result of secondary, exploratory analyses, we are hesitant to over-interpret this novel result, which needs to be replicated in future confirmatory research. We offered a tentative interpretation that such RSFC changes may reflect improved cognitive function as an idea for further exploration.

This study provides evidence of training-related changes following practice with mindfulness meditation in brain networks important for executive control and modulation of mind-wandering with relevant outcomes in self-reported attention. Individual differences in practice time and structural changes associated with PCC–DLPFC RSFC changes suggest the importance of continued practice beyond the formal instruction period. Future research to examine potential longer-term changes may need to consider factors that contribute to adopting mindfulness meditation practice as a lifestyle change, similar to the need for continued exercise and healthy eating for maintenance of healthy weight. Potential avenues to facilitate long-term use of mindfulness meditation practice may be through tailoring practices for incorporation into activities of daily living, availability of ongoing training exercises, greater accessibility of training support through mobile platforms and a meditation community. Given the wide use and efficacy of MBSR for treating numerous mental health conditions (Goldberg *et al.*, 2018), as well as the growing evidence of behaviorally-relevant biological changes as described in this study, the future of mindfulness meditation research should aim to determine factors that predict lasting change.

Conflicts of interest

Dr Richard J. Davidson is the founder, president and serves on the board of directors for the non-profit organization, Healthy Minds Innovations, Inc. No donors, either anonymous or identified, have participated in the design, conduct or reporting of research results in this manuscript.

Funding

Acknowledgements

References

Agosta, F., Pievani, M., Geroldi, C., Copetti, M., Frisoni, G.B., Filippi, M. (2012). Resting state fMRI in Alzheimer's disease: beyond the default mode network. *Neurobiology of Aging*, **33**, 1564–78 doi:https://doi.org/10.1016/j.neurobiolaging.2011.06.007.

Alexander, A.L., Lee, J.E., Lazar, M., Field, A.S. (2007). Diffusion tensor imaging of the brain. *Neurotherapeutics*, **4**, 316–29 doi:https://doi.org/10.1016/j.nurt.2007.05.011.

Andersson, J.L.R., Sotiropoulos, S.N. (2016). An integrated approach to correction for off-resonance effects and subject movement in diffusion MR imaging. *NeuroImage*, **125**, 1063–78 doi:https://doi.org/10.1016/j.neuroimage.2015.10.019.

Andrews-Hanna, J.R., Reidler, J.S., Sepulcre, J., Poulin, R., Buckner, R.L. (2010). Functional-anatomic fractionation of the brain's default network. *Neuron*, **65**, 550–62 doi:https://doi.org/10.1016/j.neuron.2010.02.005.

Avants, B., Gee, J.C. (2004). Geodesic estimation for large deformation anatomical shape averaging and interpolation. *NeuroImage*, **23**, S139–50 doi:https://doi.org/10.1016/j.neuroimage.2004.07.010.

Barrett, L.F., Satpute, A.B. (2013). Large-scale brain networks in affective and social neuroscience: towards an integrative functional architecture of the brain. *Current Opinion in Neurobiology*, **23**, 361–72 doi:https://doi.org/10.1016/j.conb.2012.12.012.

Basser, P.J., Jones, D.K. (2002). Diffusion-tensor MRI: theory, experimental design and data analysis—a technical review. *NMR in Biomedicine*, **15**, 456–67 doi:https://doi.org/10.1002/nbm.783.

Basser, P.J., Pierpaoli, C. (1996). Microstructural and physiological features of tissues elucidated by quantitative-diffusion-tensor MRI. *Journal of Magnetic Resonance*, **111**, 209–19 doi:https://doi.org/10.1006/jmrb.1996.0086.

Beaulieu, C. (2002). The basis of anisotropic water diffusion in the nervous system—a technical review. *NMR in Biomedicine*, **15**, 435–55 doi:https://doi.org/10.1002/nbm.782.

Brewer, J.A., Worhunsky, P.D., Gray, J.R., Tang, Y.-Y., Weber, J., Kober, H. (2011). Meditation experience is associated with differences in default mode network activity and connectivity. *Proceedings of the National Academy of Sciences of the United States of America*, **108**, 20254–9 doi:https://doi.org/10.1073/pnas.1112029108.

Chang, L.-C., Jones, D.K., Pierpaoli, C. (2005). RESTORE: robust estimation of tensors by outlier rejection. *Magnetic Resonance in Medicine*, **53**, 1088–95 doi:https://doi.org/10.1002/mrm.20426.

Christoff, K., Gordon, A.M., Smallwood, J., Smith, R., Schooler, J.W. (2009). Experience sampling during fMRI reveals default network and executive system contributions to mind wandering. *Proceedings of the National Academy of Sciences of the United States of America*, **106**, 8719–24 doi:https://doi.org/10.1073/pnas.0900234106.

Christoff, K., Irving, Z.C., Fox, K.C.R., Spreng, R.N., Andrews-Hanna, J.R. (2016). Mind-wandering as spontaneous thought: a dynamic framework. *Nature Reviews. Neuroscience*, **17**, 718–31 doi:https://doi.org/10.1038/nrn.2016.113.

Cox, R.W. (1996). AFNI: software for analysis and visualization of functional magnetic resonance neuroimages. *Computers and Biomedical Research*, **29**, 162–73 doi:https://doi.org/10.1006/cbmr.1996.0014.

Craddock, R.C., James, G.A., Holtzheimer, P.E., Hu, X.P., Mayberg, H.S. (2012). A whole brain fMRI atlas generated via spatially constrained spectral clustering. *Human Brain Mapping*, **33**, 1914–28 doi:https://doi.org/10.1002/hbm.21333.

Creswell, J.D., Taren, A.A., Lindsay, E.K., et al. (2016). Alterations in resting-state functional connectivity link mindfulness meditation with reduced Interleukin-6: a randomized controlled trial. *Biological Psychiatry*, **80**, 53–61 doi:https://doi.org/10.1016/j.biopsych.2016.01.008.

Curtin, J. (2015). lmSupport: support for linear models.

Fox, K.C.R., Dixon, M.L., Nijeboer, S., et al. (2016). Functional neuroanatomy of meditation: a review and meta-analysis of 78 functional neuroimaging investigations. *Neuroscience and Biobehavioral Reviews*, **65**, 208–28 doi:https://doi.org/10.1016/j.neubiorev.2016.03.021.

Garyfallidis, E., Brett, M., Amirbekian, B., et al. (2014). Dipy, a library for the analysis of diffusion MRI data. *Frontiers in Neuroinformatics*, **8**, 8 doi:https://doi.org/10.3389/fninf.2014.00008.

Goldberg, S.B., Tucker, R.P., Greene, P.A., et al. (2018). Mindfulness-based interventions for psychiatric disorders: a systematic review and meta-analysis. *Clinical Psychology Review*, **59**, 52–60 doi:https://doi.org/10.1016/j.cpr.2017.10.011.

Greve, D.N., Fischl, B. (2009). Accurate and robust brain image alignment using boundary-based registration. *NeuroImage*, **48**, 63–72 doi:https://doi.org/10.1016/j.neuroimage.2009.06.060.

Han, Y., Wang, J., Zhao, Z., et al. (2011). Frequency-dependent changes in the amplitude of low-frequency fluctuations in amnestic mild cognitive impairment: a resting-state fMRI study. *NeuroImage*, **55**, 287–95 doi:https://doi.org/10.1016/j.neuroimage.2010.11.059.

Jain, S., Shapiro, S.L., Swanick, S., et al. (2007). A randomized controlled trial of mindfulness meditation versus relaxation training: effects on distress, positive states of mind, rumination, and distraction. *Annals of Behavioral Medicine*, **33**, 11–21 doi:https://doi.org/10.1207/s15324796abm3301_2.

Jenkinson, M., Bannister, P., Brady, M., Smith, S. (2002). Improved optimization for the robust and accurate linear registration and motion correction of brain images. *NeuroImage*, **17**, 825–41 doi:https://doi.org/10.1006/nimg.2002.1132.

Jones, D.K., Cercignani, M. (2010). Twenty-five pitfalls in the analysis of diffusion MRI data. *NMR in Biomedicine*, **23**, 803–20 doi:https://doi.org/10.1002/nbm.1543.

Jones, D.K., Knösche, T.R., Turner, R. (2013). White matter integrity, fiber count, and other fallacies: the do's and don'ts of diffusion MRI. *NeuroImage*, **73**, 239–54 doi:https://doi.org/10.1016/j.neuroimage.2012.06.081.

Kabat-Zinn, J. (1990). *Full Catastrophe Living: The Program of the Stress Reduction Clinic at the University of Massachusetts Medical Center*, New York, NY: Delta, Random House Publishing Group.

Kesebir, P., Gasiorowska, A., Goldman, R., Hirshberg, M., Davidson, R.J. (2019). Emotional style questionnaire: a multidimensional measure of healthy emotionality. Psychological Assessment, doi: 10.1037/pas0000745. [Epub ahead of print].

Kim, C., Cilles, S.E., Johnson, N.F., Gold, B.T. (2012). Domain general and domain preferential brain regions associated with different types of task switching: a meta-analysis. *Human Brain Mapping*, **33**, 130–42 doi:https://doi.org/10.1002/hbm.21199.

Leemans, A., Jones, D.K. (2009). The B-matrix must be rotated when correcting for subject motion in DTI data. *Magnetic Resonance in Medicine*, **61**, 1336–49 doi:https://doi.org/10.1002/mrm.21890.

MacCoon, D.G., Imel, Z.E., Rosenkranz, M.A., *et al.* (2012). The validation of an active control intervention for mindfulness based stress reduction (MBSR). *Behaviour Research and Therapy*, **50**, 3–12 doi:https://doi.org/10.1016/j.brat.2011.10.011.

MacDonald, A.W., Cohen, J.D., Stenger, V.A., Carter, C.S. (2000). Dissociating the role of the dorsolateral prefrontal and anterior cingulate cortex in cognitive control. *Science*, **288**, 1835–8 doi:https://doi.org/10.1126/science.288.5472.1835.

Mason, M.F., Norton, M.I., Horn, J.D.V., Wegner, D.M., Grafton, S.T., Macrae, C.N. (2007). Wandering minds: the default network and stimulus-independent thought. *Science*, **315**, 393–5 doi:https://doi.org/10.1126/science.1131295.

McLaughlin, K., Travers, B.G., Dadalko, O.I., *et al.* (2018). Longitudinal development of thalamic and internal capsule microstructure in autism spectrum disorder. *Autism Research*, **11**, 450–62 doi:https://doi.org/10.1002/aur.1909.

Mori, S., Wakana, S., Zijl, P.C.M.V., Nagae-Poetscher, L.M. (2005). *MRI Atlas of Human White Matter*, Amsterdam, Elsevier.

Mrazek, M.D., Franklin, M.S., Phillips, D.T., Baird, B., Schooler, J.W. (2013). Mindfulness training improves working memory capacity and GRE performance while reducing mind wandering. *Psychological Science*, **24**, 776–81 doi:https://doi.org/10.1177/0956797612459659.

Petrides, M., Pandya, D.N. (1999). Dorsolateral prefrontal cortex: comparative cytoarchitectonic analysis in the human and the macaque brain and corticocortical connection patterns. *The European Journal of Neuroscience*, **11**, 1011–36 doi:https://doi.org/10.1046/j.1460-9568.1999.00518.x.

Power, J.D., Mitra, A., Laumann, T.O., Snyder, A.Z., Schlaggar, B.L., Petersen, S.E. (2014). Methods to detect, characterize, and remove motion artifact in resting state fMRI. *NeuroImage*, **84**, 320–41 doi:https://doi.org/10.1016/j.neuroimage.2013.08.048.

Ptak, R. (2012). The frontoparietal attention network of the human brain: action, saliency, and a priority map of the environment. *The Neuroscientist*, **18**, 502–15 doi:https://doi.org/10.1177/1073858411409051.

R Core Team. (2015). R: a language and environment for statistical computing, Vienna, Austria: R Foundation for Statistical Computing.

Smallwood, J., Brown, K., Baird, B., Schooler, J.W. (2012). Cooperation between the default mode network and the frontal–parietal network in the production of an internal train of thought. *Brain Research*, **1428**, 60–70 doi:https://doi.org/10.1016/j.brainres.2011.03.072.

Smith, S.M. (2002). Fast robust automated brain extraction. *Human Brain Mapping*, **17**, 143–55 doi:https://doi.org/10.1002/hbm.10062.

Smith, S.M., Jenkinson, M., Woolrich, M.W., *et al.* (2004). Advances in functional and structural MR image analysis and implementation as FSL. *NeuroImage*, **23**, S208–19 doi:https://doi.org/10.1016/j.neuroimage.2004.07.051.

Spreng, R.N., Grady, C.L. (2009). Patterns of brain activity supporting autobiographical memory, prospection, and theory of mind, and their relationship to the default mode network. *Journal of Cognitive Neuroscience*, **22**, 1112–23 doi:https://doi.org/10.1162/jocn.2009.21282.

Spreng, R.N., Sepulcre, J., Turner, G.R., Stevens, W.D., Schacter, D.L. (2013). Intrinsic architecture underlying the relations among the default, dorsal attention, and frontoparietal control networks of the human brain. *Journal of Cognitive Neuroscience*, **25**, 74–86, doi:https://doi.org/10.1162/jocn_a_00281.

Winkler, A.M., Ridgway, G.R., Webster, M.A., Smith, S.M., Nichols, T.E. (2014). Permutation inference for the general linear model. *NeuroImage*, **92**, 381–97 doi:https://doi.org/10.1016/j.neuroimage.2014.01.060.

WMA (2013). The world medical association—WMA declaration of Helsinki—ethical principles for medical research involving human subjects *JAMA*, **310**: 2191–4. doi: 10.1001/jama.2013.281053..

Zatorre, R.J., Fields, R.D., Johansen-Berg, H. (2012). Plasticity in gray and white: neuroimaging changes in brain structure during learning. *Nature Neuroscience*, **15**, 528–36 doi:https://doi.org/10.1038/nn.3045.

Zeestraten, E.A., Benjamin, P., Lambert, C., *et al.* (2016). Application of diffusion tensor imaging parameters to detect change in longitudinal studies in cerebral small vessel disease. *PLoS One*, **11**, doi:https://doi.org/10.1371/journal.pone.0147836, e0147836.

Zeidan, F., Johnson, S.K., Diamond, B.J., David, Z., Goolkasian, P. (2010). Mindfulness meditation improves cognition: evidence of brief mental training. *Consciousness and Cognition*, **19**, 597–605 doi:https://doi.org/10.1016/j.concog.2010.03.014.

Zhang, H., Yushkevich, P.A., Alexander, D.C., Gee, J.C. (2006). Deformable registration of diffusion tensor MR images with explicit orientation optimization. *Medical Image Analysis*, **10**, 764–85 doi:https://doi.org/10.1016/j.media.2006.06.004.